

AD-A244 344



AD

TECHNICAL REPORT ARCCB-TR-91034

**MATERIALS ANALYSIS OF A
FATIGUE TESTING MANDREL**

**M. BRODSKY
J. SENICK
G. YOUNG**

92-01316



NOVEMBER 1991



**US ARMY ARMAMENT RESEARCH,
DEVELOPMENT AND ENGINEERING CENTER
CLOSE COMBAT ARMAMENTS CENTER
BENÉT LABORATORIES
WATERVLIET, N.Y. 12189-4050**



APPROVED FOR PUBLIC RELEASE; DISTRIBUTION UNLIMITED

92 1 15 004

DISCLAIMER

The findings in this report are not to be construed as an official Department of the Army position unless so designated by other authorized documents.

The use of trade name(s) and/or manufacturer(s) does not constitute an official indorsement or approval.

DESTRUCTION NOTICE

For classified documents, follow the procedures in DoD 5200.22-M, Industrial Security Manual, Section II-19 or DoD 5200.1-R, Information Security Program Regulation, Chapter IX.

For unclassified, limited documents, destroy by any method that will prevent disclosure of contents or reconstruction of the document.

For unclassified, unlimited documents, destroy when the report is no longer needed. Do not return it to the originator.

REPORT DOCUMENTATION PAGE

Form Approved
OMB No. 0704-0188

Public reporting burden for this collection of information is estimated to average 1 hour per response, including the time for reviewing instructions, searching existing data sources, gathering and maintaining the data needed, and completing and reviewing the collection of information. Send comments regarding this burden estimate or any other aspect of this collection of information, including suggestions for reducing this burden, to Washington Headquarters Services, Directorate for Information Operations and Reports, 1215 Jefferson Davis Highway, Suite 1204, Arlington, VA 22202-4302, and to the Office of Management and Budget, Paperwork Reduction Project (0704-0188), Washington, DC 20503.

1. AGENCY USE ONLY (Leave blank)		2. REPORT DATE November 1991	3. REPORT TYPE AND DATES COVERED Final	
4. TITLE AND SUBTITLE MATERIALS ANALYSIS OF A FATIGUE TESTING MANDREL			5. FUNDING NUMBERS AMCMS No. 6126.23.1BL0.0 PRON No. 1A92ZMGWNMSC	
6. AUTHOR(S) M. Brodsky, J. Senick, and G. Young				
7. PERFORMING ORGANIZATION NAME(S) AND ADDRESS(ES) U.S. Army ARDEC Benet Laboratories, SMCAR-CCB-TL Watervliet, NY 12189-4050			8. PERFORMING ORGANIZATION REPORT NUMBER ARCCB-TR-91034	
9. SPONSORING / MONITORING AGENCY NAME(S) AND ADDRESS(ES) U.S. Army ARDEC Close Combat Armaments Center Picatinny Arsenal, NJ 07806-5000			10. SPONSORING / MONITORING AGENCY REPORT NUMBER	
11. SUPPLEMENTARY NOTES				
12a. DISTRIBUTION / AVAILABILITY STATEMENT Approved for public release; distribution unlimited.			12b. DISTRIBUTION CODE	
13. ABSTRACT (Maximum 200 words) A metallurgical analysis was conducted on a fatigue testing mandrel that failed abruptly in service after 5061 cycles. The mode of failure was identified as fatigue, and most mechanical property values were determined to be far below the minimum specifications for marage 250 steel. Degradation of the material properties of the mandrel, resulting in a decreased fatigue life, was attributed to improper processing of the material.				
14. SUBJECT TERMS Mandrel, Fatigue, Marage 250 Steel, Mechanical Properties			15. NUMBER OF PAGES 31	
			16. PRICE CODE	
17. SECURITY CLASSIFICATION OF REPORT UNCLASSIFIED	18. SECURITY CLASSIFICATION OF THIS PAGE UNCLASSIFIED	19. SECURITY CLASSIFICATION OF ABSTRACT UNCLASSIFIED	20. LIMITATION OF ABSTRACT UL	

TABLE OF CONTENTS

	<u>Page</u>
INTRODUCTION	1
PROCEDURE	1
RESULTS	2
Magnetic Particle Inspection	2
Ultrasonic Testing	2
Stereoscopic/Visual Examination	2
Measurement of Radius	3
Chemical Analysis	4
Hardness Measurement	4
Microstructural Evaluation	4
Experimental Heat Treatments	5
Microhardness Measurement	5
Mechanical Property Testing	5
X-Ray Diffraction Analysis	6
Scanning Electron Microscopy/Energy Dispersive Spectroscopy	6
CONCLUSIONS	8
RECOMMENDATIONS	9
REFERENCES	10

TABLES

I. CHEMICAL ANALYSIS	11
II. MECHANICAL PROPERTY ANALYSIS	12

LIST OF ILLUSTRATIONS

1. Failed fatigue testing mandrel, as-received	13
2a. Photograph of fracture surface showing concentric rings	14

2b. Crescent-shaped indication and ridges found on fracture surface, as-received	14
2c. Photograph of fracture surface exhibiting ridges, wood chips, and crescent and crack indications, as-received	15
2d. Perimeter of fracture surface depicting crack, crescent, and notch indications, as-received	15
3a. Fracture surface of fatigue testing mandrel, post-cleaned condition	16
3b. Photograph showing indications discovered on fracture surface, post-cleaned condition	16
4a. Longitudinal view of fracture surface showing depth of secondary crack	17
4b. High magnification view of secondary crack found in mandrel	17
5. Schematic of fatigue testing mandrel showing location of failure	18
6a. Photomicrograph illustrating transverse view of microstructure of as-received marage 250 steel	19
6b. High magnification view showing martensitic microstructure	19
7a. SEM fractograph showing fatigue striations discovered on fracture surface	20
7b. Fatigue striations found on fracture surface	20
7c. High magnification fractograph of fatigue striations	21
7d. Ductile rupture discovered in center region of fracture surface	21
8a. Fractograph showing secondary crack and large indication	22
8b. Large indication and secondary crack discovered on fracture surface	22
9a. Fractograph of secondary crack showing intergranular cracking	23

9b. Fractograph of secondary crack showing intergranular cracking	23
10. SEM micrograph showing globular and elongated particles	24
11. EDS analysis of globular particle	25
12. EDS analysis of elongated particle	26
13a. SEM fractograph showing the shear lip and fracture region of longitudinal tensile test bar	27
13b. SEM fractograph depicting ductile appearance of longitudinal tensile test bar	27
14a. SEM fractograph illustrating ductile rupture discovered in longitudinal Charpy impact bar	28
14b. SEM fractograph showing microvoid coalescence and titanium-rich particles found in longitudinal Charpy impact bar	28

Accession For	
NTIS GRA&I	<input checked="" type="checkbox"/>
DTIC TAB	<input type="checkbox"/>
Unannounced	<input type="checkbox"/>
Justification	<input type="checkbox"/>
By	
Date	
Dist	
A-1	

INTRODUCTION

A materials characterization and failure analysis was performed on a fatigue testing mandrel that failed abruptly in service after a total of only 5061 cycles. The mandrel was reportedly composed of marage 250 grade steel, and the raw material was specified to be delivered in the solution-annealed condition. Subsequent processing was to include rough machining to the approximate mandrel dimensions, an aging treatment at 900°F for four hours, and finish machining.

PROCEDURE

The failed mandrel was examined according to the following procedure:

1. Magnetic particle inspection
2. Ultrasonic testing
3. Stereoscopic/visual examination
4. Measurement of radius
5. Chemical analysis
6. Hardness measurement
7. Microstructural evaluation
8. Experimental heat treatments
9. Microhardness measurement
10. Mechanical property testing
 - a. Tensile
 - b. Charpy impact toughness
 - c. Fracture toughness (K_{IC})
 - d. Fatigue crack growth
11. X-ray diffraction analysis
12. Scanning electron microscopy/energy dispersive spectroscopy

RESULTS

Magnetic Particle Inspection

Magnetic particle examination was performed on both mating fracture surfaces of the subject mandrel, as well as the entire machined surface, as shown in Figure 1, to determine the presence of macroscopic crack indications. No indications were found along the outside finish-machined surface. Large indications, however, were discovered along the outer perimeter of the fracture surface, adjacent to the finish-machined circumferential surfaces, as shown in Figure 2a.

Ultrasonic Testing

Ultrasonic inspection was performed on the machined surfaces of mating mandrel pieces to determine the existence and degree of any surface or subsurface discontinuities. No additional indications were discovered by this test, nor was the depth of the indication found on the fracture surface determined.

Stereoscopic/Visual Examination

A visual analysis was initially performed on the as-received mandrel as shown in Figures 1 through 2d. The fracture surface, which was then cleaned with acetone, is shown in the post-cleaned condition in Figures 3a and 3b.

Upon general inspection by both visual and stereoscopic means, several prominent surface features were observed. First, as shown in Figure 2a, the overall fracture surface appeared to be divided into three roughly concentric rings: a relatively smooth outer ring of 3/8 inch maximum width (R1) bounded by the finish-machined surface and a circumferential indication, then a slightly coarser, shiny ring of 3/4 inch maximum width (R2), and finally the inner circle (R3) of 3 3/4 inches maximum diameter, noticeably darker in color and covered with ridges. Located between R2 and R3 were two crescent-shaped indications

approximately 1/2 inch by 2 inches and 3/8 inch by 1 1/4 inches, as shown in Figure 3a. Both of these were traced by the directions of the ridges found on the surface of the inner circle, as illustrated in Figure 3b. Also shown in this figure are two additional niche-shaped indications of approximately 1/4 inch by 1/4 inch and 3/8 inch by 1/4 inch maximum, which were discovered in R1 along the finish-machined surface. As seen in this figure, the indications were located behind the large crescent. All of these observations are characteristic features commonly associated with the progressive nature of fatigue failures.

In order to determine the depth of the circumferential indication exhibited in Figure 2a, it was necessary to divide one of the mating fracture surfaces of the mandrel in half. Figures 4a and 4b show the longitudinal plane of the fracture surface that clearly identifies the circumferential indication as a crack. These figures also show the depth and severity of this crack. In addition, the crack was measured and determined to extend a maximum of approximately 1 3/8 inches into the mandrel at a 45-degree angle to the transverse plane. Note in Figure 4a that the crack extends from both sides of the fracture surface, and that the various depths of this crack are virtually equal to the depth of the striated region of the primary crack leading to failure. A similar secondary crack exists at the same location in the mating half of the mandrel, which also extends at 45-degree angles from the fracture surface and 90-degree angles from the previously mentioned secondary crack.

Measurement of Radius

The mandrel fractured at the sharpest radius point as shown in Figure 5. When a post-failure inspection was performed on this area, the radius was measured and the average was determined to be 0.030 inch. This measurement,

although within specifications of $0.03R + 0.01$, was at the low end of the requirement, making this radius the sharpest acceptable within the above limits.

Chemical Analysis

The results of the chemical analysis are shown in Table I. All values are in accordance with the specifications for marage 250 steel with the exception of silicon. A value slightly in excess of the requirement was obtained. However, this deviation is considered to be insignificant and within the limits of experimental error.

Hardness Measurement

Rockwell hardness measurements (HRC) were taken across the entire mandrel diameter. Results obtained were in the 40 to 42 HRC range, which was significantly lower than the required 48 to 52 HRC specified.

At the time these results were obtained, we attempted to acquire both the Watervliet Arsenal and vendor heat treat records to verify whether this material was given the proper thermal heat treatments. This proved futile, as there were no heat treat records or any written documentation pertaining to this particular mandrel material. Consequently, we were unable to verify whether this material was processed correctly by either the vendor or Watervliet Arsenal.

Microstructural Evaluation

The results of our microstructural evaluation are shown in Figures 6a and 6b. These photomicrographs reveal a homogeneous, predominantly martensitic structure typical of maraging steels. In addition, the coarse-grained appearance of the microstructure is indicative of a material that underwent a solution treatment at a relatively high temperature and/or was solution treated for a long period of time.

Experimental Heat Treatments

Experimental heat treatments were performed on this material in an attempt to determine its thermal history. The procedure consisted of underaging, properly aging, and overaging samples of this material at temperatures of 800°F, 900°F, and 1000°F, respectively, to simulate the observed microstructure and resulting hardness of the as-received mandrel. Although this was unsuccessful, we were able to obtain the required hardness of 49 HRC for the specimen which was re-annealed and aged at 900°F. In addition, when a portion of the as-received material was aged for three hours at 900°F, it also attained the required hardness of 49 HRC. However, we found no sources that could verify that the proper microstructure of either specimen was also attained.

Microhardness Measurement

In addition to Rockwell hardness testing, Knoop microhardness measurements were taken, also on a transverse section of the mandrel. Results in the 40 to 42 HRC range were obtained, thus corroborating earlier findings from the Rockwell tester.

Mechanical Property Testing

The results of extensive mechanical property testing are shown in Table II. The material was found to be primarily isotropic, with the exception of fracture toughness, and the overall results obtained were far below minimum requirements.

All mechanical properties in the longitudinal direction, with the exception of elongation, were significantly below minimum requirements. The yield strength was approximately 70 Ksi below the required value, while the tensile strength was deficient by about 40 Ksi. In addition, toughness properties were sharply lower than expected, impact energy results were at half the specified value, and fracture toughness values were about $30 \text{ Ksi}\sqrt{\text{in.}}$ lower. The lowest

fracture toughness value was found in the orientation plane where the crack was located. Once again, these results indicate that the mechanical property condition of this mandrel did not meet specified requirements.

Fatigue crack growth studies were also performed utilizing specimens machined from the failed mandrel. In this substandard material, it was approximated that a crack would initiate at 1750 cycles and propagate an additional 3625 cycles to failure, giving an overall life of 5375 cycles. These data are in accordance with ASTM test method E647-88a on "Measurement of Fatigue Crack Growth Rates" (ref 1). These results are remarkably close to the actual failure rate of 5061 cycles! However, the life expectancy of a mandrel fabricated from standard marage 250 steel was calculated at 40,000 cycles. This indicates that the crack was initiating and propagating at a significantly faster rate than originally predicted.

X-Ray Diffraction Analysis

X-ray diffraction techniques were used to determine the percentage of martensite versus austenite present in the microstructure of the mandrel. The purpose of this analysis was threefold. First, the presence of austenite in sufficient quantities would facilitate a path for rapid crack propagation. Second, it would also explain the low hardness of the material. Third, this test was also used to verify microstructural constituents revealed through metallography. However, diffraction results indicated that the mandrel material contained a fully martensitic structure with essentially no austenite present.

Scanning Electron Microscopy/Energy Dispersive Spectroscopy

Scanning electron microscopy (SEM) was used to characterize the fracture surface of the mandrel. The most prevalent feature discovered throughout the outer two rings, R1 and R2, was the presence of fatigue striations, depicted in

Figures 7a through 7c. In contrast, the center region of the fracture surface displayed rather ductile characteristics, as shown in Figure 7d.

Figures 8a and 8b illustrate one of the niche-shaped indications and the circumferential crack. This indication may have been an initiation site for the primary (fatigue) crack. Since fatigue was present in substantial amounts, this crack likely propagated to critical size by this mechanism. As stated earlier, two secondary cracks were found propagating at 45-degree angles to both the fatigue crack and the transverse plane. One crack was opened for examination. Figures 9a and 9b depict the fracture surface and the intergranular nature of this crack.

Energy dispersive spectroscopy (EDS) was conducted on the metallographic samples, and the two particle types that were analyzed are displayed in Figure 10. The results in Figure 11 show that the bright, globular-shaped particles are titanium-rich, common to maraging steels, while the elongated particles are additionally rich in molybdenum as illustrated in Figure 12.

Figures 13a, 13b, 14a, and 14b reflect the SEM investigation of tensile and Charpy test bars, respectively. At low magnification, the tensile test bar appeared to have a coarse, granular-type appearance in the fracture region. Upon closer investigation, the fracture mode was identified as microvoid coalescence, characteristic of a ductile material, as was the Charpy fractograph shown in Figure 14a. Figure 14b depicts a magnified region of a Charpy bar that contained several titanium particles. These particles were found sparsely distributed throughout the ductile fracture surface.

CONCLUSIONS

Common characteristics of fatigue including concentric rings, ridges, and a relatively flat, shiny appearance were discovered on the fracture surface of the failed mandrel. A circumferential crack located near the finish-machined surface of the mandrel was also found. Also apparent in this area were two niche-shaped indications that may have been the crack initiation sites.

Three different cracks were contained in the subject mandrel. The primary crack propagated by fatigue and the secondary cracks were attributed to a combination of intergranular and fatigue fracture mechanisms.

SEM analysis confirmed fatigue as the crack propagation mechanism over the outer two concentric rings on the fracture surface, while the inner fast fracture region showed characteristics of ductile rupture.

A fully martensitic structure, showing no indications of reverted or retained austenite, was revealed by both metallographic and x-ray diffraction techniques. Also discovered was the presence of titanium carbonitrides, $Ti(C,N)$ precipitates, which result from the age-hardening process.

Mechanical property test results revealed values far below minimum specifications. Substandard hardness and strength values were the primary material property deficiencies that led to the reduced fatigue life of this mandrel.

Since there were no receipt records of this material from the vendor or any heat treat records, there was no viable way to trace the processing history of this steel. Consequently, it was not possible to determine the exact processing operation that caused the degradation of the material properties of this marage 250 steel to the above extremes.

RECOMMENDATIONS

To avoid similar problems in the future involving fatigue testing mandrels with deficient mechanical properties, it is imperative that a post-heat treatment hardness check be instituted. This will minimize the possibility of improperly processed material entering service. It is also suggested that more accurate receipt and material processing records be documented. Furthermore, we suggest periodic magnetic particle in-service inspections in the following order: post-fabrication, after the mandrel has been in service for 3,000 cycles, and subsequently every 1,000 cycles. The mandrel should be retired at the instant cracking is exhibited during inspection.

REFERENCES

1. "Measurement of Fatigue Crack Growth Rates. ASTM E-647-88a," Annual Book of ASTM Standards, Vol. 3.01, American Society for Testing and Materials, Philadelphia, PA, 1989, pp. 647-666.

TABLE I. CHEMICAL ANALYSIS*

	Benet	Required
Nickel	17.8	17.0-19.0
Cobalt	8.3	7.0-8.5
Molybdenum	4.7	4.6-5.2
Titanium	0.45	0.3-0.5
Aluminum	0.07	0.05-0.15
Carbon	0.026	0.03 Max
Manganese	0.008	0.10 Max
Silicon	0.110	0.10 Max
Phosphorus	0.005	0.01 Max
Sulfur	0.000	0.01 Max
Iron	Bal	Bal

*Weight percent

TABLE II. MECHANICAL PROPERTY ANALYSIS

	Benet		Required	
	Longitudinal	Tranverse	Longitudinal	Transverse
Yield strength 0.2 % offset, Ksi	176-178	176-177	240 Min	216 Min
Ultimate tensile strength, Ksi	197-198	198	-	-
Elongation, %	7.9-13.8	9.7-10.6	6.0 Min	5.4 Min
Impact toughness -40°F, ft-lbs	9	10-26	18 Min	16.2 Min
Fracture toughness K_{Ic} , Ksi $\sqrt{\text{in.}}$	67-75	106	100 Min	90 Min

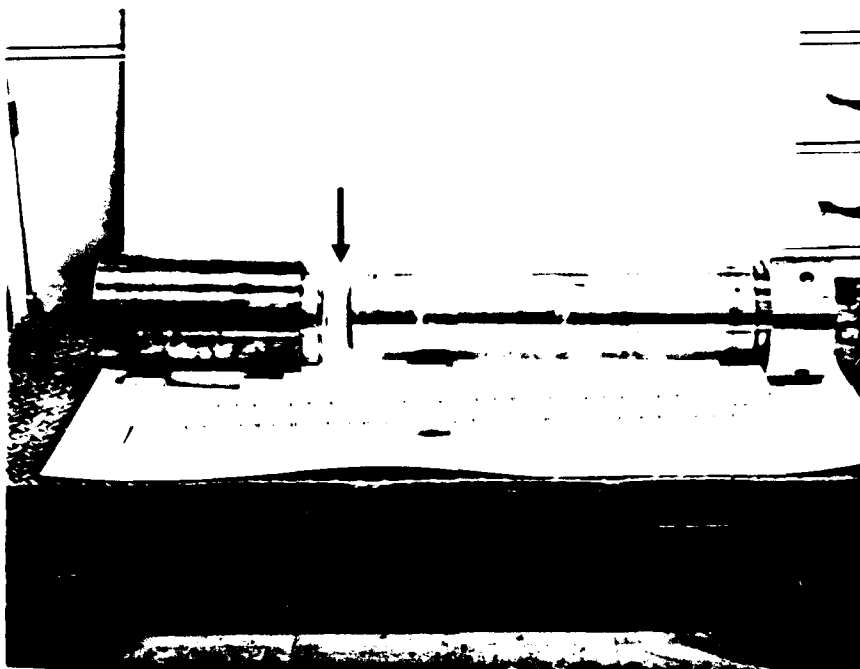


Figure 1. Failed fatigue testing mandrel,
as-received (scale in inches).



Figure 2a. Photograph of fracture surface showing concentric rings, as-received.

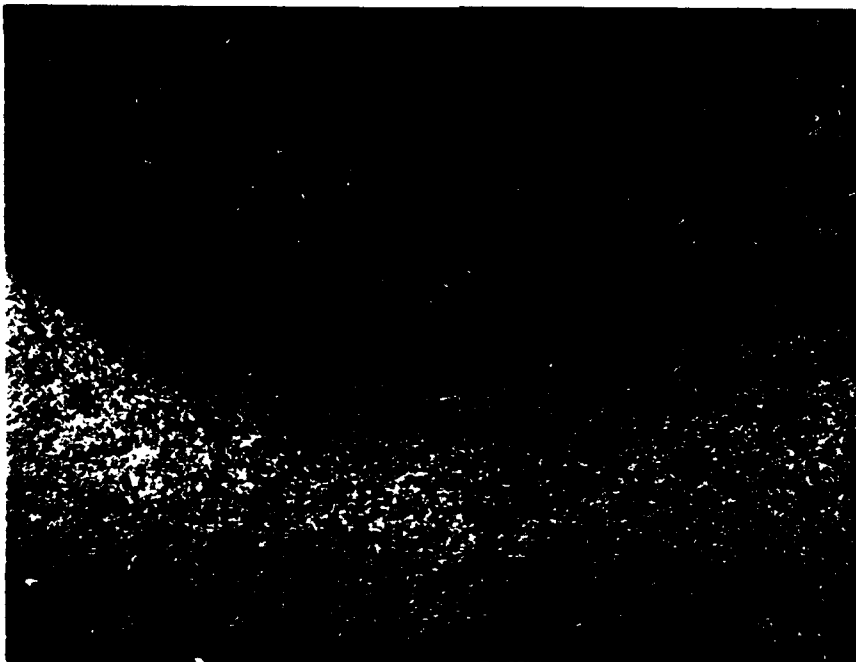


Figure 2b. Crescent-shaped indication and ridges found on fracture surface, as-received.



Figure 2c. Photograph of fracture surface exhibiting bridges, wood chips, and crescent and crack indications, as-received.

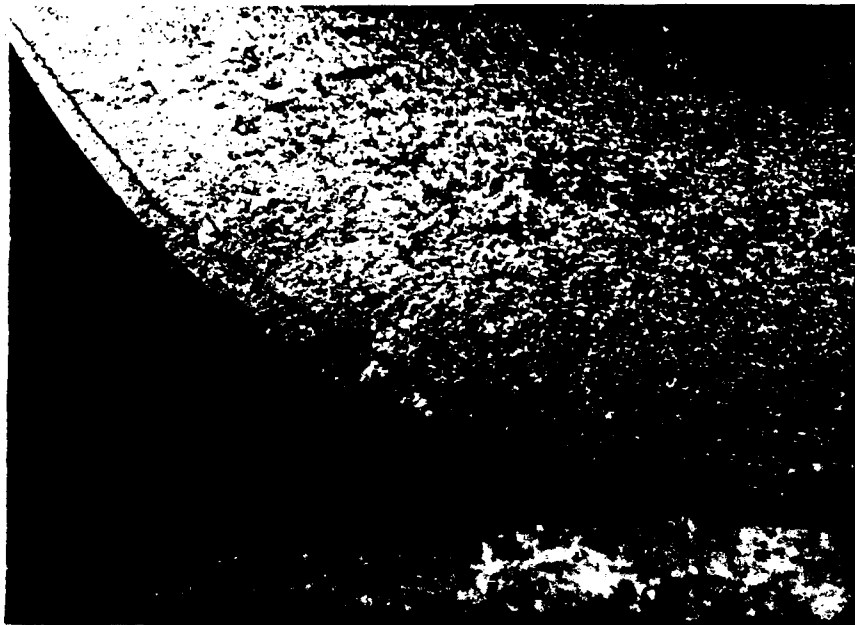


Figure 2d. Perimeter of fracture surface depicting crack, crescent, and notch indications, as-received.

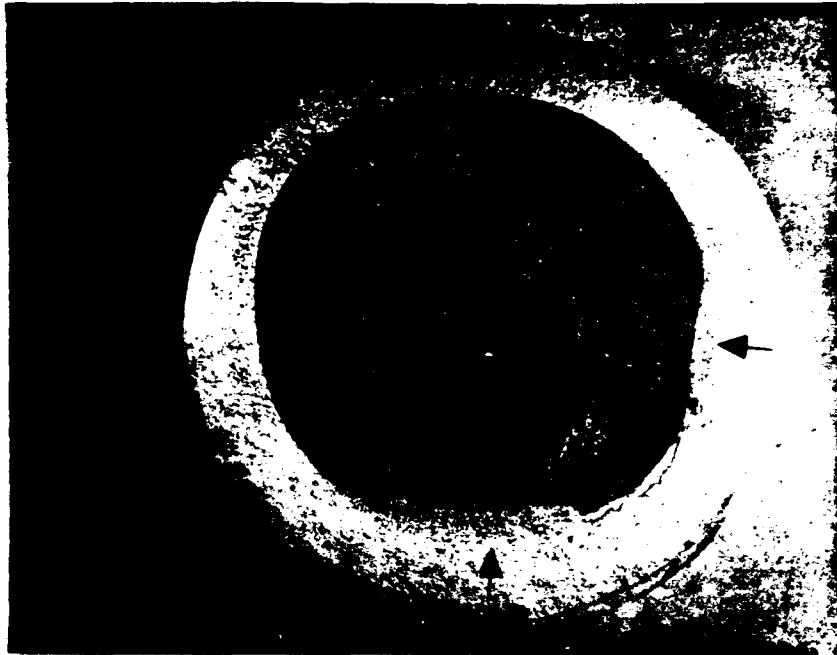


Figure 3a. Fracture surface of fatigue testing mandrel, post-cleaned condition.



Figure 3b. Photograph showing indications discovered on fracture surface, post-cleaned condition.

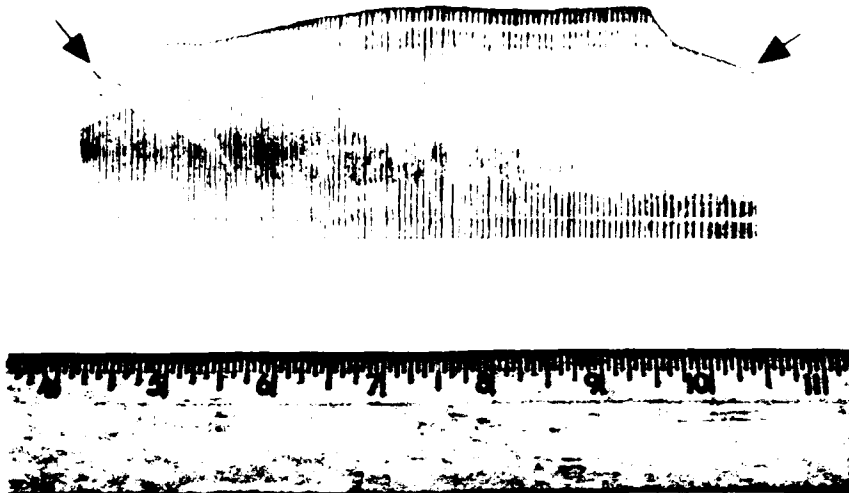


Figure 4a. Longitudinal view of fracture surface showing depth of secondary crack.



Figure 4b. High magnification view of secondary crack found in mandrel.

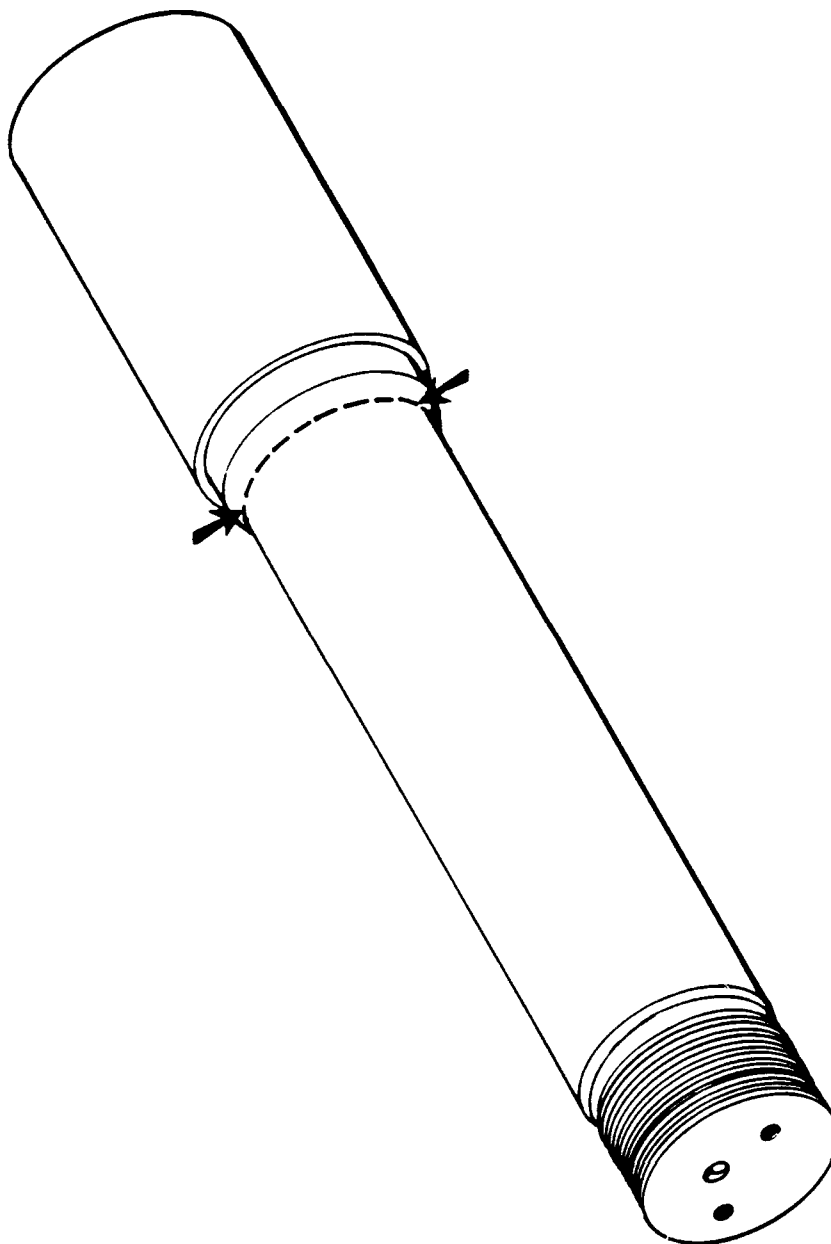


Figure 5. Schematic of fatigue testing mandrel showing location of failure.



Figure 6a. Photomicrograph illustrating transverse view of microstructure of as-received marage 250 steel. Etchant - Fry's reagent (200X).



Figure 6b. High magnification view showing martensitic microstructure. Etchant - Fry's reagent (1000X).

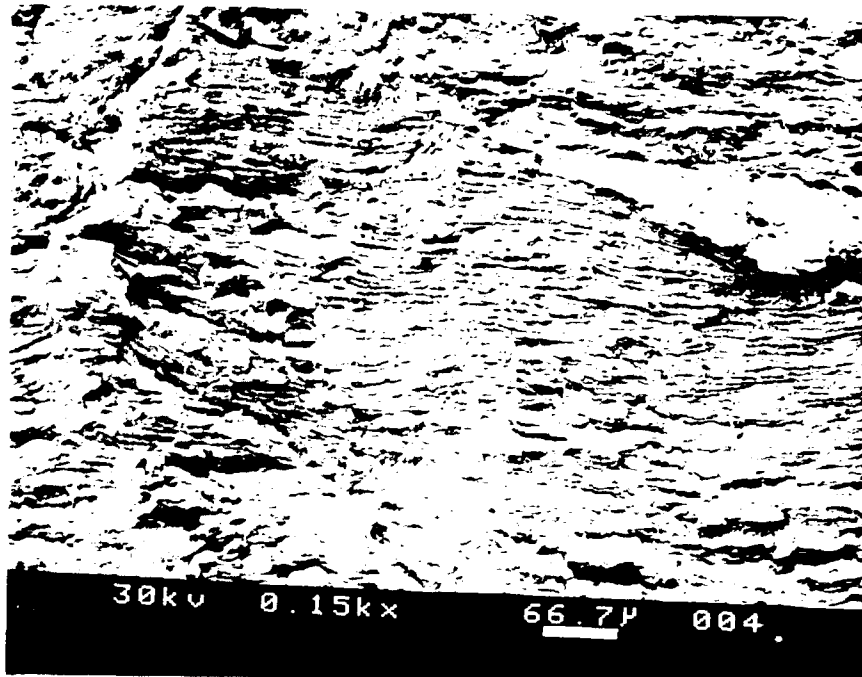


Figure 7a. SEM fractograph showing fatigue striations discovered on fracture surface. Backscatter emission (150X).

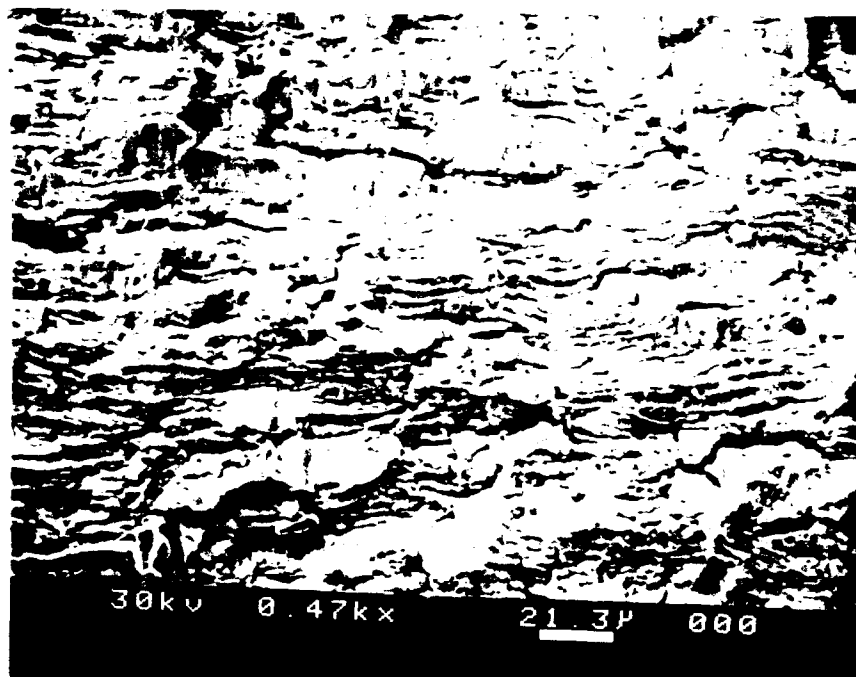


Figure 7b. Fatigue striations found on fracture surface. Backscatter emission (470X).

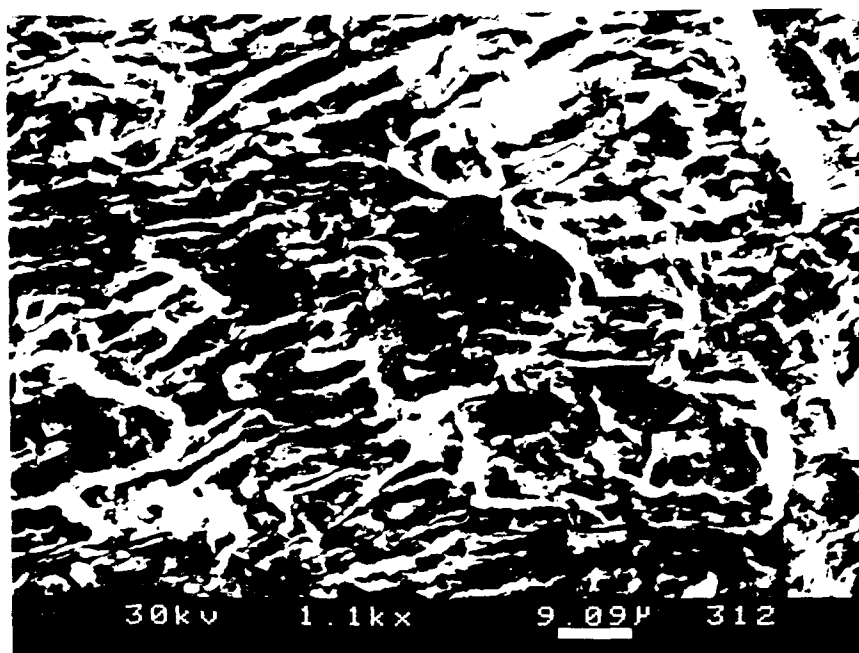


Figure 7c. High magnification fractodograph of fatigue striations. Secondary emission (1100X).

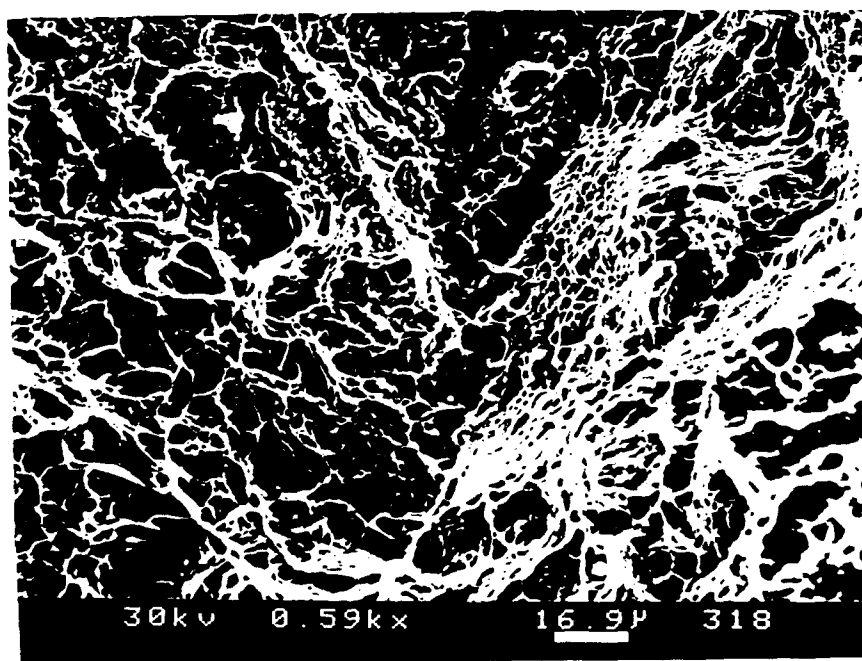


Figure 7d. Ductile rupture discovered in center region of fracture surface. Secondary emission (590X).

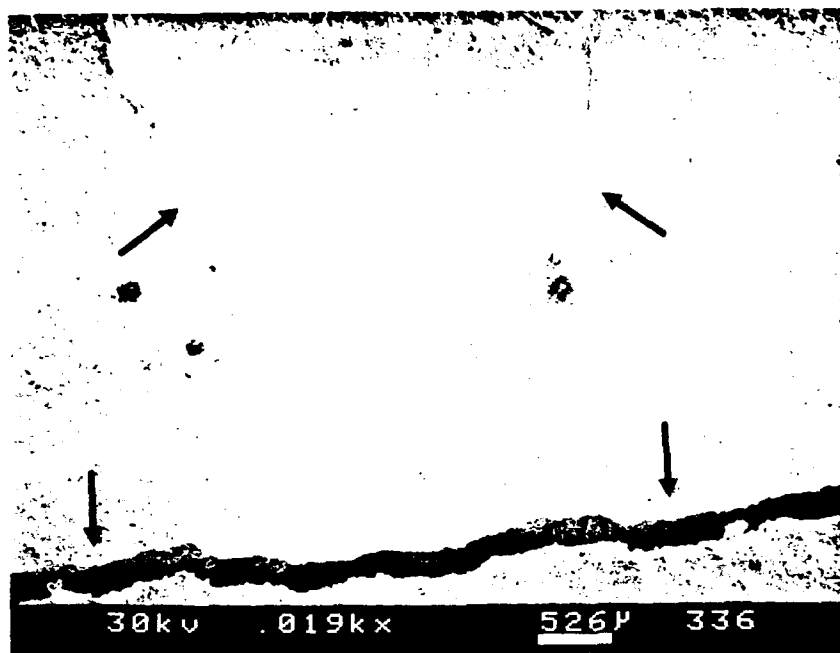


Figure 8a. Fractograph showing secondary crack and large indication. Secondary emission (19X).

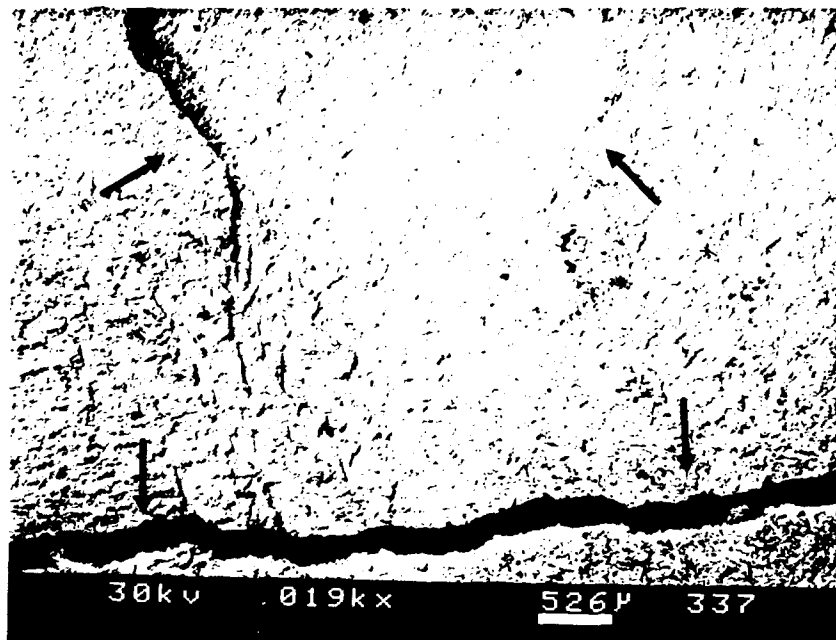


Figure 8b. Large indication and secondary crack discovered on fracture surface. Backscatter emission (19X).

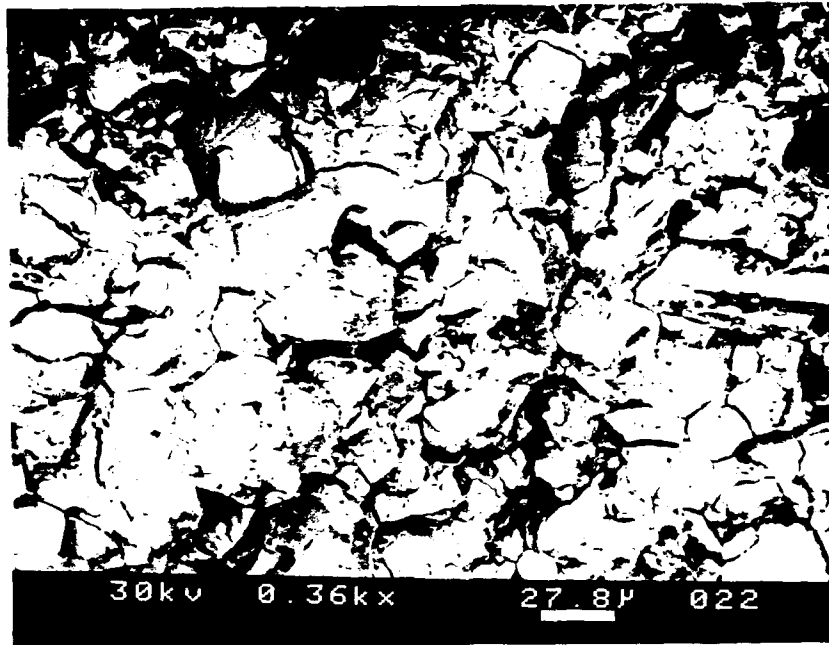


Figure 9a. Fractograph of secondary crack showing intergranular cracking. Backscatter emission (360X).

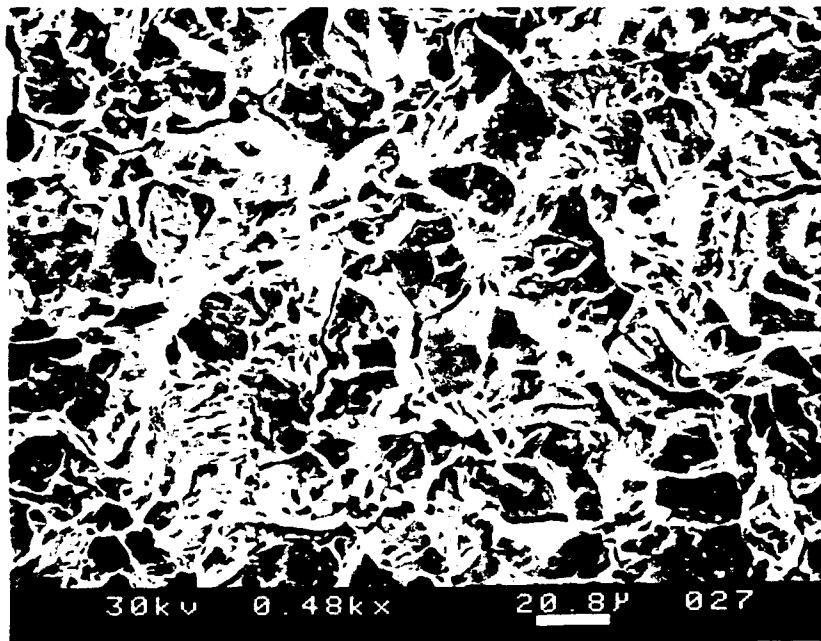


Figure 9b. Fractograph of secondary crack showing intergranular cracking. Secondary emission (480X).

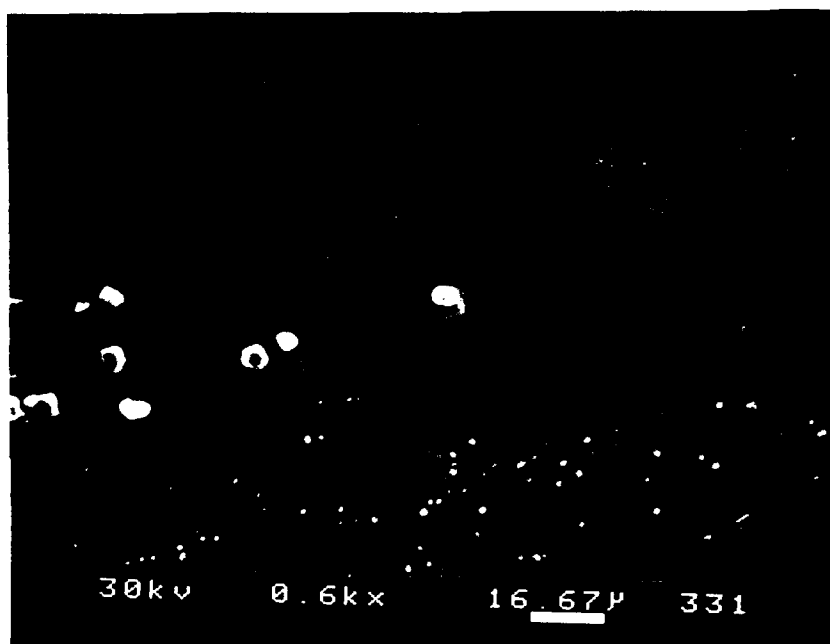


Figure 10. SEM micrograph showing globular and elongated particles. Backscatter emission (600X).

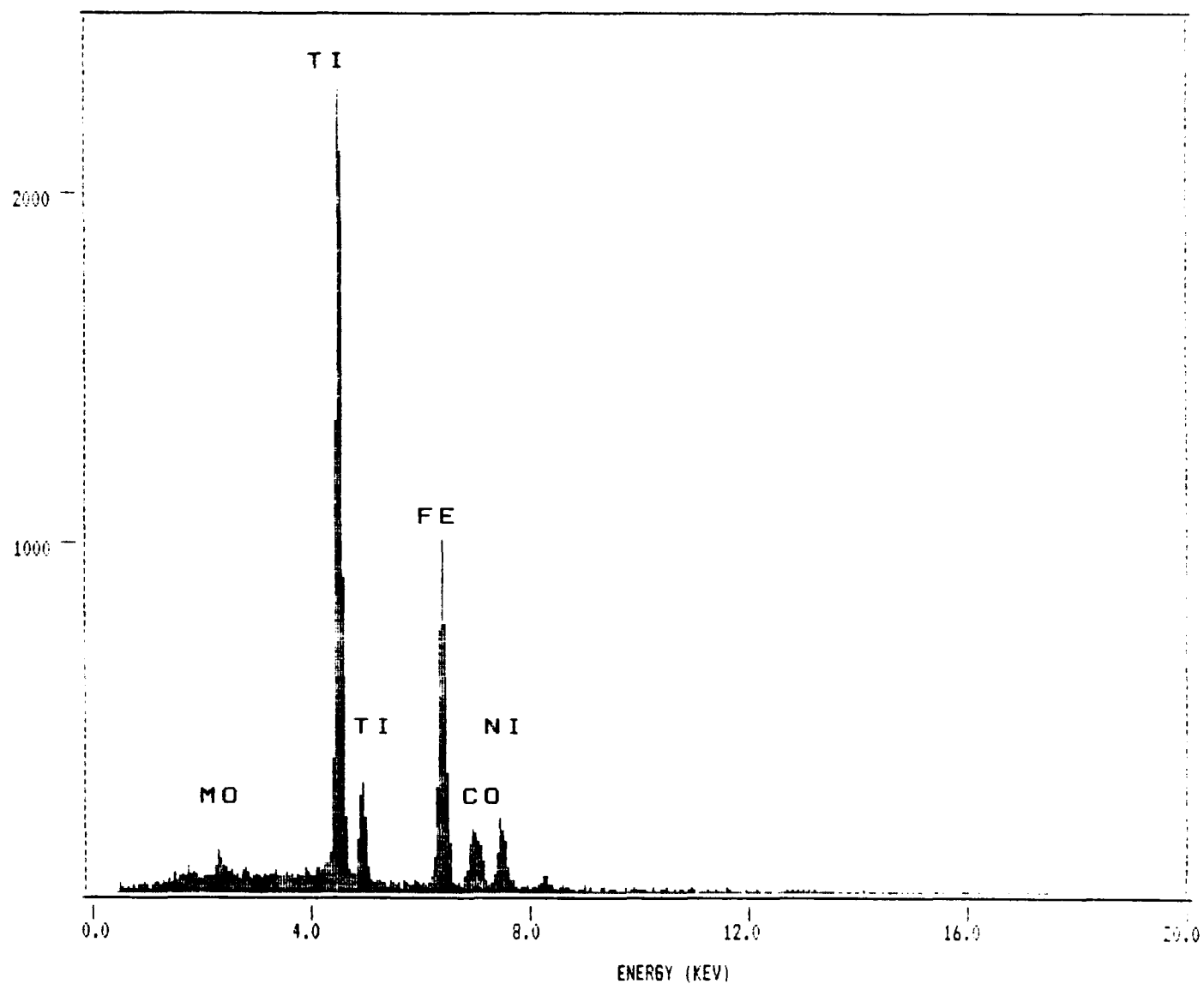
PARTICLE A

SPECTRUM LABEL

120MM XM 291 MANDREL

SPECTRUM FILE NAME

MANDREL



8P16ITI

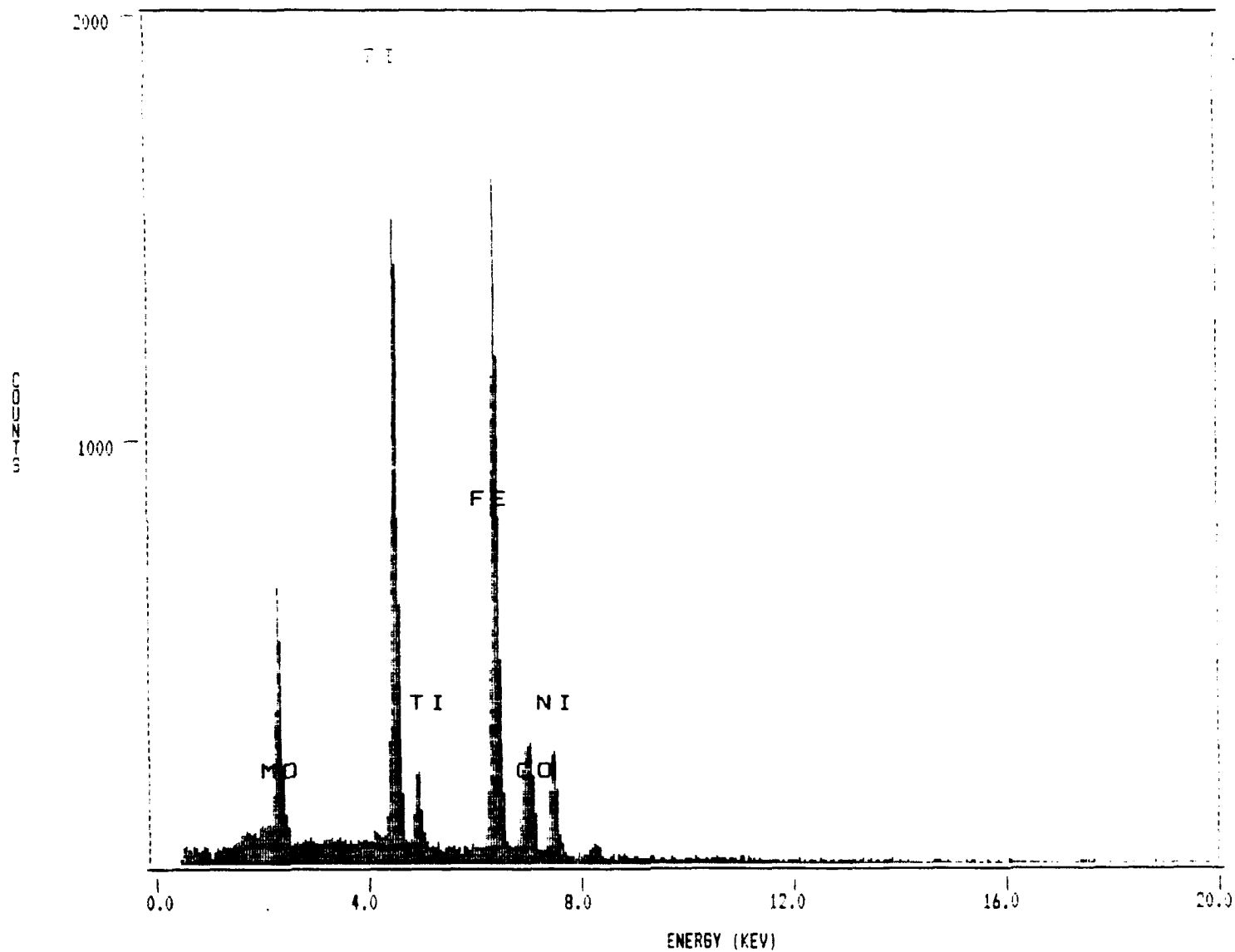
Figure 11. EDS analysis of globular particle.

ELONGATED PARTICLE

SPECTRUM LABEL

SPECTRUM FILE NAME

120MM CM 291 MANDREL



8P1611

Figure 12. EDS analysis of elongated particle.

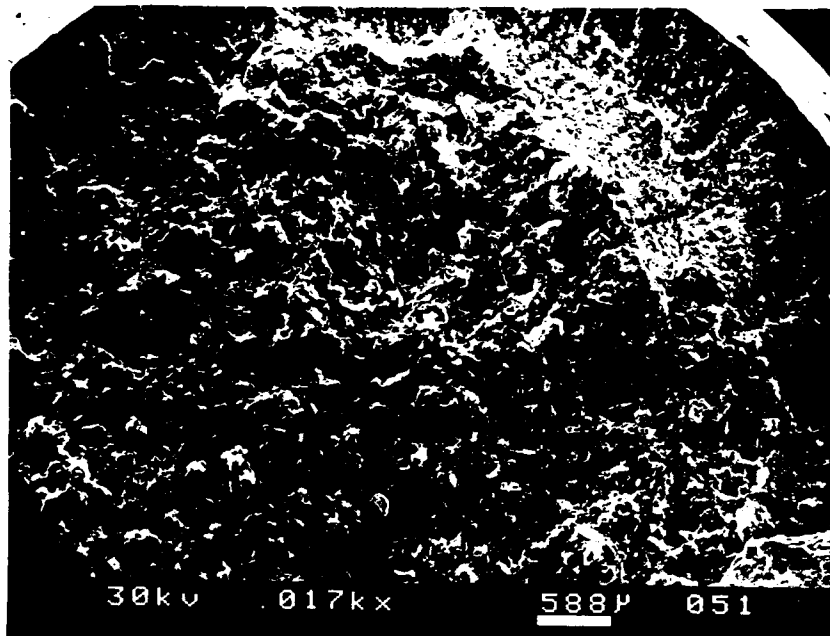


Figure 13a. SEM fractograph showing the shear lip and fracture region of longitudinal tensile test bar. Secondary emission (17X).

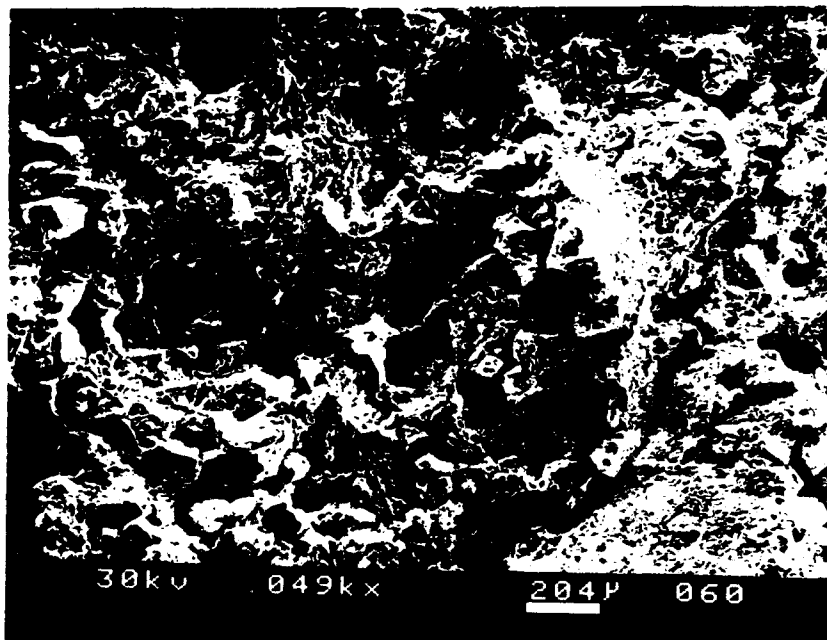


Figure 13b. SEM fractograph depicting ductile appearance of longitudinal tensile test bar. Secondary emission (49X).

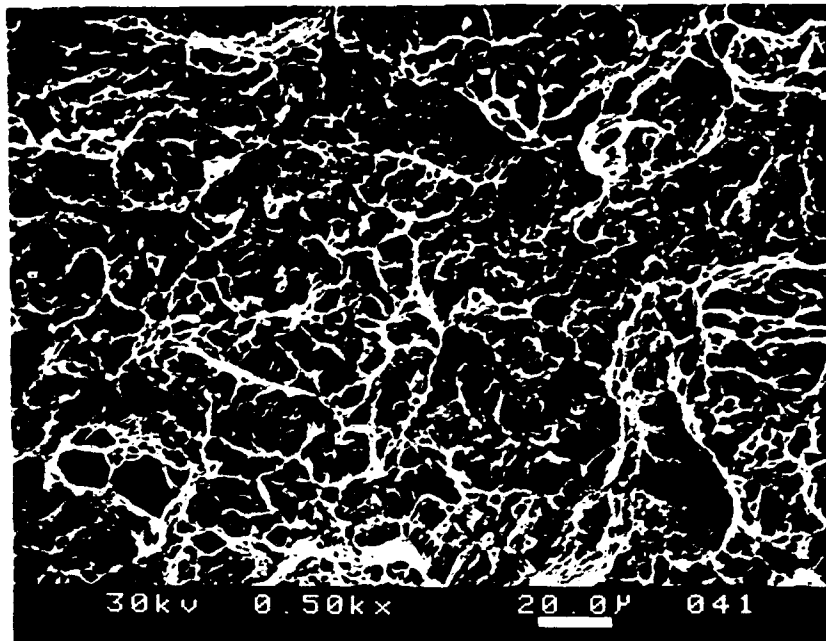


Figure 14a. SEM fractograph illustrating ductile rupture discovered in longitudinal Charpy impact bar. Secondary emission (500X).

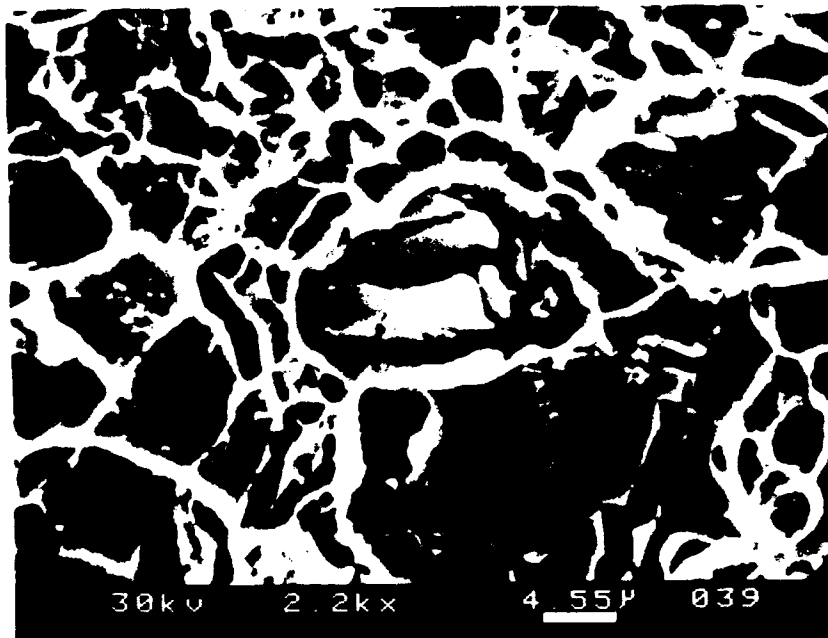


Figure 14b. SEM fractograph showing microvoid coalescence and titanium-rich particles found in longitudinal Charpy impact bar. Secondary emission (2200X).

TECHNICAL REPORT INTERNAL DISTRIBUTION LIST

	NO. OF COPIES
CHIEF, DEVELOPMENT ENGINEERING DIVISION	
ATTN: SMCAR-CCB-DA	1
-DC	1
-DI	1
-DR	1
-DS (SYSTEMS)	1
CHIEF, ENGINEERING SUPPORT DIVISION	
ATTN: SMCAR-CCB-S	1
-SD	1
-SE	1
CHIEF, RESEARCH DIVISION	
ATTN: SMCAR-CCB-R	2
-RA	1
-RE	1
-RM	1
-RP	1
-RT	1
TECHNICAL LIBRARY	
ATTN: SMCAR-CCB-TL	5
TECHNICAL PUBLICATIONS & EDITING SECTION	
ATTN: SMCAR-CCB-TL	3
OPERATIONS DIRECTORATE	
ATTN: SMCWV-ODP-P	1
DIRECTOR, PROCUREMENT DIRECTORATE	
ATTN: SMCWV-PP	1
DIRECTOR, PRODUCT ASSURANCE DIRECTORATE	
ATTN: SMCWV-QA	1

NOTE: PLEASE NOTIFY DIRECTOR, BENET LABORATORIES, ATTN: SMCAR-CCB-TL, OF ANY ADDRESS CHANGES.

TECHNICAL REPORT EXTERNAL DISTRIBUTION LIST

	<u>NO. OF COPIES</u>		<u>NO. OF COPIES</u>
ASST SEC OF THE ARMY RESEARCH AND DEVELOPMENT ATTN: DEPT FOR SCI AND TECH THE PENTAGON WASHINGTON, D.C. 20310-0103	1	COMMANDER ROCK ISLAND ARSENAL ATTN: SMCRI-ENM ROCK ISLAND, IL 61299-5000	1
ADMINISTRATOR DEFENSE TECHNICAL INFO CENTER ATTN: DTIC-FDAC CAMERON STATION ALEXANDRIA, VA 22304-6145	12	DIRECTOR US ARMY INDUSTRIAL BASE ENGR ACTV ATTN: AMXIB-P ROCK ISLAND, IL 61299-7260	1
COMMANDER US ARMY ARDEC ATTN: SMCAR-AEE	1	COMMANDER US ARMY TANK-AUTMV R&D COMMAND ATTN: AMSTA-DDL (TECH LIB) WARREN, MI 48397-5000	1
SMCAR-AES, BLDG. 321	1	COMMANDER	
SMCAR-AET-O, BLDG. 351N	1	US MILITARY ACADEMY	1
SMCAR-CC	1	ATTN: DEPARTMENT OF MECHANICS	
SMCAR-CCP-A	1	WEST POINT, NY 10996-1792	
SMCAR-FSA	1		
SMCAR-FSM-E	1	US ARMY MISSILE COMMAND	
SMCAR-FSS-D, BLDG. 94	1	REDSTONE SCIENTIFIC INFO CTR	2
SMCAR-IMI-I (STINFO) BLDG. 59	2	ATTN: DOCUMENTS SECT, BLDG. 4484	
PICATINNY ARSENAL, NJ 07806-5000		REDSTONE ARSENAL, AL 35898-5241	
DIRECTOR US ARMY BALLISTIC RESEARCH LABORATORY ATTN: SLCBR-DD-T, BLDG. 305	1	COMMANDER US ARMY FGN SCIENCE AND TECH CTR ATTN: DRXST-SD	1
ABERDEEN PROVING GROUND, MD 21005-5066		220 7TH STREET, N.E. CHARLOTTESVILLE, VA 22901	
DIRECTOR US ARMY MATERIEL SYSTEMS ANALYSIS ACTV ATTN: AMXSY-MP	1	COMMANDER US ARMY LABCOM	
ABERDEEN PROVING GROUND, MD 21005-5071		MATERIALS TECHNOLOGY LAB ATTN: SLCMT-IML (TECH LIB)	2
COMMANDER HQ, AMCCOM		WATERTOWN, MA 02172-0001	
ATTN: AMSMC-IMP-L	1		
ROCK ISLAND, IL 61299-6000			

NOTE: PLEASE NOTIFY COMMANDER, ARMAMENT RESEARCH, DEVELOPMENT, AND ENGINEERING CENTER, US ARMY AMCCOM, ATTN: BENET LABORATORIES, SMCAR-CCB-TL, WATERVLIET, NY 12189-4050, OF ANY ADDRESS CHANGES.

TECHNICAL REPORT EXTERNAL DISTRIBUTION LIST (CONT'D)

	NO. OF COPIES		NO. OF COPIES
COMMANDER US ARMY LABCOM, ISA ATTN: SLCIS-IM-TL 2800 POWDER MILL ROAD ADELPHI, MD 20783-1145	1	COMMANDER AIR FORCE ARMAMENT LABORATORY ATTN: AFATL/MN EGLIN AFB, FL 32542-5434	1
COMMANDER US ARMY RESEARCH OFFICE ATTN: CHIEF, IPO P.O. BOX 12211 RESEARCH TRIANGLE PARK, NC 27709-2211	1	COMMANDER AIR FORCE ARMAMENT LABORATORY ATTN: AFATL/MNF EGLIN AFB, FL 32542-5434	1
DIRECTOR US NAVAL RESEARCH LAB ATTN: MATERIALS SCI & TECH DIVISION CODE 26-27 (DOC LIB) WASHINGTON, D.C. 20375	1 1	MIAC/CINDAS PURDUE UNIVERSITY 2595 YEAGER ROAD WEST LAFAYETTE, IN 47905	1
DIRECTOR US ARMY BALLISTIC RESEARCH LABORATORY ATTN: SLCBR-IB-M (DR. BRUCE BURNS) ABERDEEN PROVING GROUND, MD 21005-5066	1		

NOTE: PLEASE NOTIFY COMMANDER, ARMAMENT RESEARCH, DEVELOPMENT, AND ENGINEERING CENTER, US ARMY AMCCOM, ATTN: BENET LABORATORIES, SMCAR-CCB-TL, WATERVLIET, NY 12189-4050, OF ANY ADDRESS CHANGES.